A&A 450, 351–358 (2006)
DOI: 10.1051/0004-6361:20054174

Astronomy & Astrophysics

The relation between Ca bright grains and oscillations in the photosphere

S. Kamio and H. Kurokawa

Kwasan and Hida Observatories, Kyoto University, Kyoto 607-8471 Japan
e-mail: kamio@kwasan.kyoto-u.ac.jp

Received 8 September 2005 / Accepted 25 November 2005

ABSTRACT

Context. Ca bright grains are small and repetitive brightenings ubiquitously found in the quiet Sun.
Aims. The relationship between the formation of Ca bright grains and the dynamics in the chromosphere and the photosphere is studied.
Methods. We simultaneously observed the time series of spectra in Ca II H, Hα, and Fe I with the horizontal spectrograph of the Domeless Solar Telescope (DST) at Hida Observatory.
Results. Our wavelet analysis revealed that the occurrence of Ca II H_{2V} brightenings are correlated with enhanced 5 mHz velocity oscillations in the chromosphere and the photosphere.
Conclusions. Ca bright grains can be explained by acoustic shocks in the chromosphere that are associated with 5 mHz oscillations in the photosphere below.

Key words. Sun: chromosphere – Sun: oscillations – Sun: photosphere

1. Introduction

As small (2–3 arcsec) transient (1 min) brightenings, Ca II H bright grains are ubiquitously found in the quiet Sun. Cram & Damé (1983) obtained Ca II H spectra with high spatial and temporal resolution and revealed the temporal behavior of Ca II H bright grains. The brightenings usually occur at 3 min intervals, so they are thought to be related to 3 min oscillations in the chromosphere. On the other hand, high velocity periodic upflow events (5 km s^{-1}) of 2–3 arcsec size have also been observed in Hα spectra (Kamio & Kurokawa 2004). They appear as small dark points in the blue wing of Hα filtergram, also at 3 min intervals. They have been called Hα dark grains in the Hα filtergram (Gaizauskas 1985). The similar nature of these two different features suggests they are different aspects of the same phenomena, but previous observations have not firmly established the relation between them.

The excellent review by Rutten & Uitenbroek (1991) suggests that grains are generated by the interference of waves in the chromosphere. Carlsson & Stein (1997) carried out a 1-D radiation-hydrodynamic simulation and claims Ca II H_{2V} bright grains were generated by acoustic shocks. They simulate the wave driven by photospheric motions and their result closely reproduces the observed characteristics of Ca II H spectra.

The purpose of our study is to examine the relationship between Ca bright grains, Hα dark grains, and velocities in the chromosphere and the photosphere. Spectra in Ca II H, Hα (or Hβ), and Fe I are simultaneously observed in order to study their temporal evolutions. We employed Hα or Hβ spectral lines to determine the velocities in the chromosphere, because the velocity derived from the Ca II H_3 dark core may be affected by the brightening in Ca II H_{2V} or H_{2R}. The long duration data sets are suitable for frequency analysis by wavelet transformation. In Sect. 2, we briefly describe the observations. Section 3 explains the data reduction procedures for the observed spectra. The evolution of photospheric and chromospheric velocities and Ca II H_{2V} intensities are presented in Sect. 4. In Sect. 5, we discuss the relationship between the formation of grains and the photospheric and chromospheric oscillations.

2. Observations

The quiet Sun near the disk center was observed by the Domeless Solar Telescope (DST) at Hida Observatory in July and August 2004. The observation was specifically aimed at studying the relationship between Ca II H brightenings and the velocities in the chromosphere and the photosphere. We utilized the horizontal spectrograph of the DST, which is capable of observing different wavelength ranges simultaneously. We mainly observed the evolution of Hα (λ656.28 nm) and Ca II H (λ396.85 nm) in the 1st order and 2nd order spectra, respectively, in sit-and-stare mode (i.e. at a fixed position without rotational compensation).

The slit was oriented in the east-west direction on the Sun, and it covered a spatial distance of about 110 Mm. The projected slit width was 0.32 arcsec or 230 km on the Sun. Pixel sizes corresponded to 0.14 Mm (on the Sun) × 1.2 pm (in wavelength) and 0.11 Mm × 2.5 pm for Ca II H and Hα, respectively. In the observation on 31 July, Hβ in the 2nd order spectra was observed instead of Hα. The pixel size for Hβ was 0.11 Mm × 1.0 pm. The entrance slit of the spectrograph was monitored with the Hα Lyot filter (0.025 nm *FWHM*) and its approximate field of view was 220 Mm × 220 Mm on the Sun. Two spectra and a slit image were recorded using three CCD cameras controlled by separate PCs with an interval of 15 s. Although the exposures of the cameras were not synchronized, temporal resolutions are enough for studying grains whose period is about 200 s. The image fluctuation on the slit plane is less than the size of grains (about 1 Mm) in good seeing conditions. The telescope was pointed at the center of the Sun, but the solar rotation was not compensated for.

The data sets obtained in good seeing conditions and without interruption were selected and their analysis is presented in this paper. Continuous observations for 1 h or longer are particularly suitable for wavelet transformation in the following analysis. In the following sections, we focus on the two selected data sets obtained on 31 July and 2 August. On 31 July, time series of Ca II H and Hβ spectra were obtained for 75 min from 22:56 UT. The exposure times were 2.0 s in Ca II H and 0.3 s in Hβ. On 2 August, a longer data set was obtained for 150 min from 23:15 UT in Ca II H and Hα with exposure times of 2.0 s and 0.3 s, respectively. Displacement due to the wavelength dependency of atmospheric refraction is estimated to be 1.1 arcsec between Ca II H and Hα spectra. Because the displacement is smaller than the typical grain size (2–3 arcsec), it is not corrected in the following study. For Ca II H and Hβ spectra, a smaller displacement of 0.7 arcsec is expected. A pair of hair lines were placed on the slit throughout the observation in order to co-align the spectra for the subsequent analysis.

3. Data reduction

The temporal evolution of spectra was studied for each location along the spectrograph slit. The wavelength in the Ca II H spectra was determined using the mean positions of Fe I lines as references (λ396.61 nm and λ396.93 nm). Intensities of Ca II H_{2V}, H_3, and H_{2R} are inferred by integrating spectra within the ranges of λ396.830–396.843 nm, λ396.843–396.856 nm, and λ396.856–396.869 nm, respectively. The Doppler velocity of the photosphere was derived by measuring the wavelength shift in the Fe I line at λ396.93 nm in the Ca II H wing. The Doppler velocity was assumed to be zero at the average position of the Fe I line. The line of sight velocity in the chromosphere was deduced from the Doppler shift of Hα or Hβ spectra. The center position of the core of the Hα (or Hβ) line profile was determined by fitting the 2nd order polynomial function. The line width is defined as the width at the half depth of the Hα or (Hβ) absorption profile (*FWHM*). The excess width relative to the average width was then used for the following analysis.

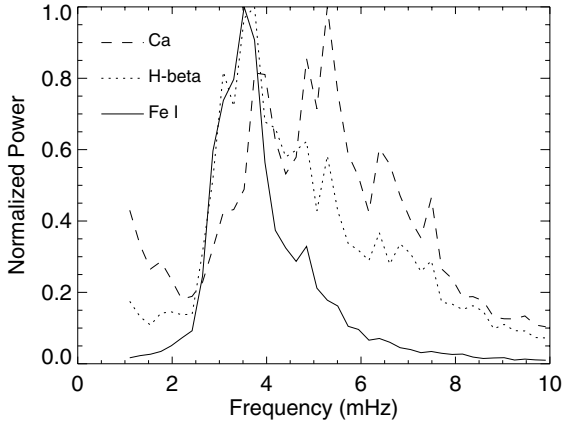

Fig. 1. Power spectrum deduced from the data on 31 July. Each spectrum is normalized by its peak. *Solid line*: power spectrum of photospheric velocity inferred from Fe I. *Dotted line*: power spectrum of chromospheric velocity deduced from Hβ. *Dashed line*: power spectrum of Ca II H_{2V} intensity.

In order to study temporal evolutions of Ca II H_{2V} intensity and of the chromospheric and photospheric velocities deduced from Hα (or Hβ) and Fe I, wavelet transformations were applied to all the data. Wavelet analysis is suitable for determining the occurrence of a transient oscillation and its frequency. The duration of the wavelet window was set to 500 s, which can cover 2 cycles of typical grains. The wavelet analysis was performed at each position on the slit, so the analysis produced a three-dimensional data array (position × time × frequency).

4. Results

4.1. Data set on 31 July

First, power spectra of photospheric and chromospheric velocities and Ca II H_{2V} intensity are deduced by Fourier transformation. While the wavelet transformation in the following analysis is aimed at identifying sporadic oscillations, Fourier transformation provides the average power spectrum over the whole data set. Figure 1 shows power spectra of Fe I velocity, Hβ velocity, and Ca II H_{2V} intensity. The strongest power of photospheric velocity inferred from Fe I is found at 3.5 mHz, which is commonly referred to as the 5-min oscillation in the photosphere. The strongest peak is also found in the power spectrum of Hβ velocity. In the frequency range higher than 4 mHz, the Hβ power spectrum indicates a stronger power than Fe I. In the power spectrum of Ca II H_{2V} intensity, the strongest power is found at 5 mHz. Even though a strong power of 3–4 mHz is found, higher frequency powers also exist in the chromosphere (5–8 mHz).

Figure 2 shows the time series of Ca II H spectra on 31st July at a fixed location where typical Ca II H bright grains were observed. Repeated Ca II H_{2V} brightenings are found at λ396.84 nm with an interval of about 3 min. The duration of individual brightening was less than 1 min. The temporal behavior of Ca II H spectra agrees with previous observations (Cram & Damé 1983; Rutten & Uitenbroek 1991). After an H_{2V} brightening, the dark H_3 core (λ396.85 nm at rest)

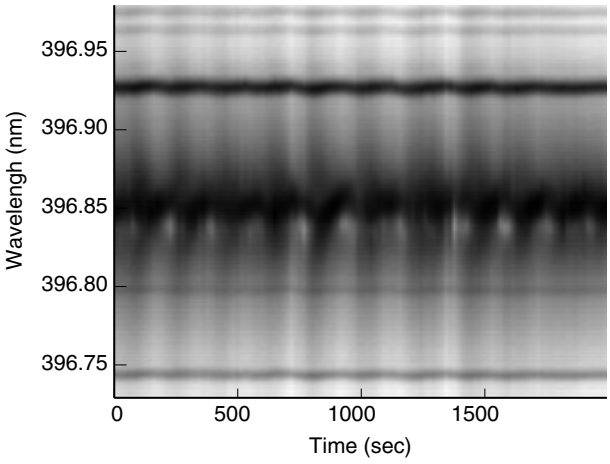

Fig. 2. Time series of Ca II H spectra at a fixed position showing bright grains. Repetitive brightenings in Ca II H_{2V} around 396.84 nm show typical grains. The Fe I line at λ396.93 nm is used to derive the velocity in the photosphere.

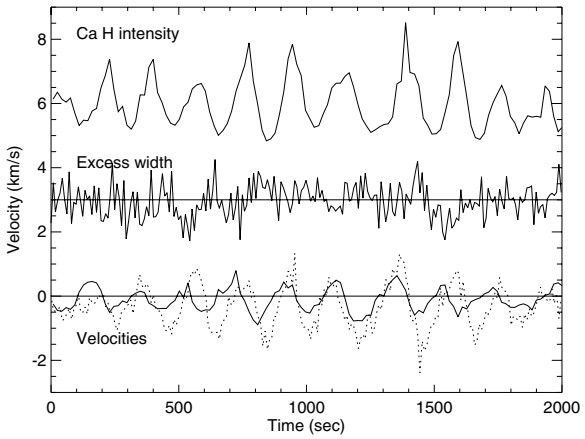

Fig. 3. Time plot of Ca II H_{2V} intensity, Hβ excess line width, and velocities. The uppermost curve shows Ca II H_{2V} intensity. The solid curve in the middle indicates the excess line width of Hβ relative to the average width, which is denoted by the straight horizontal line in the middle. The dotted and solid lines in the lower part of the figure are the velocity curves derived from Hβ and Fe I, respectively. Positive velocity indicates downward motion onto the solar surface.

exhibits a rapid blue-shift, which implies an upward motion. The wings gradually become brighter as the H_3 core goes back to its nominal position. The H_{2V} brightening occurs when the H_3 core indicates a red-shift. While Ca H_{2V} shows noticeable brightenings, significant brightenings are not found in H_{2R}.

For the data set of Fig. 2, Ca II H_{2V} intensity, the excess line width of Hβ and the velocity inferred from Hβ and Fe I are plotted in Fig. 3. The downward peak of the photospheric velocity derived from Fe I precedes that of the chromospheric velocity inferred from Hβ by 30 s on average. The intensity peak in Ca II H_{2V} is attained when Hβ indicates maximum downward velocity. The line width of Hβ tends to broaden from the increasing to the maximum phase of Hβ upward velocity. It suggests the existence of turbulence in the chromosphere when the downward motion changes to the upward motion. The Ca H_{2V} light curve and velocity curves indicate periodic

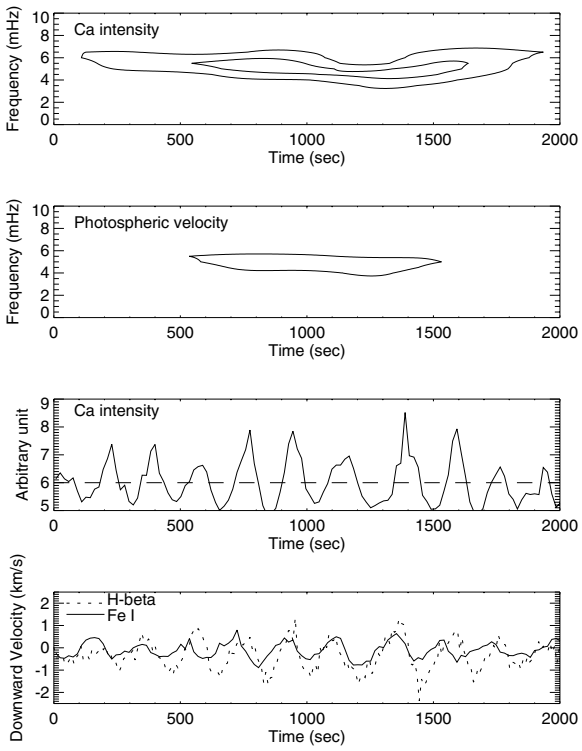

Fig. 4. *Top 2 panels*: contours of power spectra deduced by wavelet transformation of Ca II H_{2V} intensity and photospheric velocity. *Bottom panels*: light curve in Ca II H_{2V}, velocities in Hβ (dotted line), and Fe I (solid line), which are the same as in Fig. 3.

oscillations of about 200 s. While the strongest Fe I oscillatory power is found at 3.5 mHz in the average power spectrum in Fig. 1, the Fe I velocity shows quasi-periodic oscillations of about 200 s (5 mHz) in Fig. 3 when Ca II H_{2V} bright grains are observed.

The result of wavelet analysis of the same data set is presented in Fig. 4. It shows the temporal change of power spectra at the fixed slit position. The spectra implies that strong power is distributed in the frequency range of 4–6 mHz both for Ca II H_{2V} intensity and photospheric velocity. These results suggest that periodic Ca II H_{2V} brightening is associated with the high frequency oscillation (4–6 mHz) in the photosphere below.

However, the photosphere is dominated by a 5-min oscillation, and the high frequency oscillation is less significant on average (Fig. 1). In order to examine whether the high frequency oscillation in the photosphere is related to the one in the chromosphere, the location and the time of the significant high frequency oscillation in the photosphere is determined with the aid of wavelet transformation.

Figure 5 shows the photospheric velocity deduced from Fe I. Oscillatory motions can be found everywhere on the map, but the amplitude of the oscillation is not uniformly distributed. From the result of wavelet transformation, the distribution of oscillatory power in 5 mHz is retrieved to identify the location of high frequency oscillations in the photosphere. The overlaid contour in Fig. 5 marks the time and position of

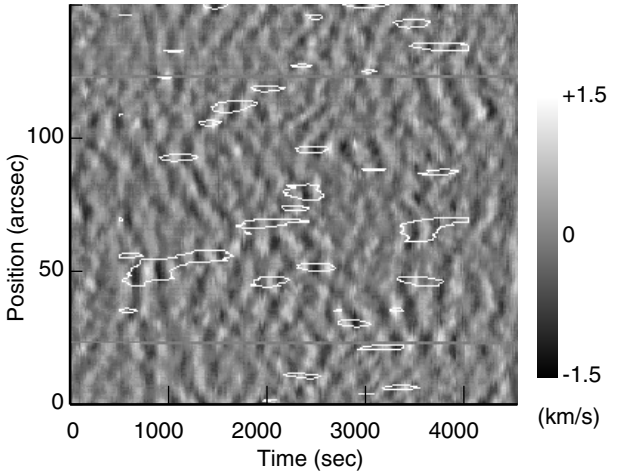

Fig. 5. The evolution of the velocity derived from Fe I. Downward and upward velocities appear bright and dark, respectively. Overlaid white contours indicate significant oscillatory power at 5 mHz.

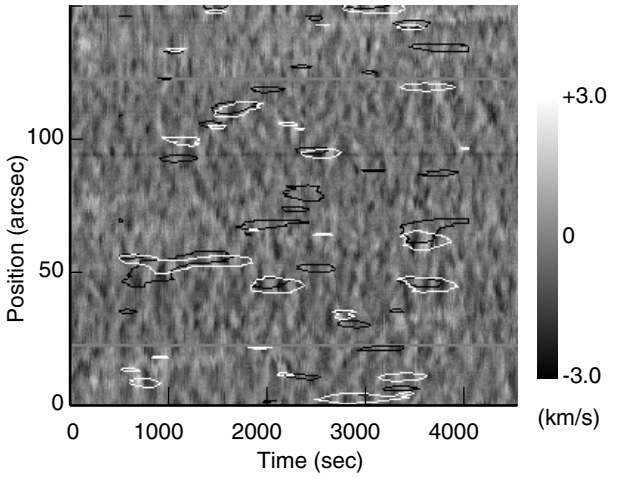

Fig. 6. The evolution of the velocity derived from Hβ. White and black contours mark significant 5 mHz power in Hβ and in Fe I, respectively. The time range is the same as in Fig. 5.

strong power in 5 mHz. The contour level is set to 2σ above the mean in the power distribution.

The velocity derived from Hβ is presented in Fig. 6. Although Hβ is not purely chromospheric and is partly photospheric, Hβ represents the higher part of the atmosphere than does Fe I. Overlaid white contours indicate the strong 5 mHz oscillatory power derived from the Hβ velocity. Black contours show the locations with significant 5 mHz oscillatory power in the photosphere that were identified in Fig. 5. From visual inspection, most of the Hβ contours are associated with Fe I contours. The cross correlation between 5 mHz power distributions in Fe I and in Hβ is 0.57. This implies that the high frequency oscillation in the chromosphere is indeed connected with that in the photosphere.

Figure 7 shows the Ca II H_{2V} intensity distribution. Overlaid white contours mark the strong intensity oscillations at 5 mHz. Black contours show a significant 5 mHz oscillatory power in Hβ identified in Fig. 6. The figure clearly shows that the high frequency oscillation in Ca II H_{2V} intensity is well

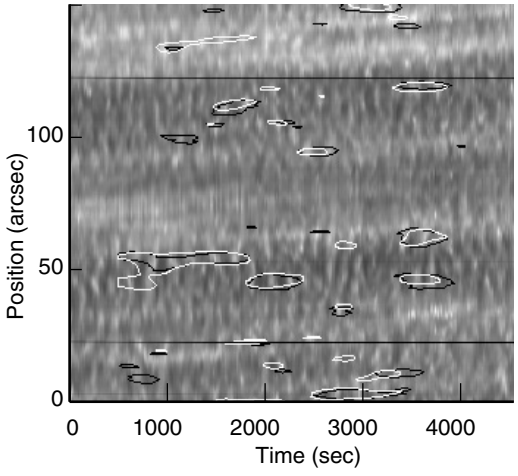

Fig. 7. The evolution of Ca II H_{2V} intensity. White and black contours indicate significant 5 mHz power in Ca II H_{2V} intensity and in Hβ velocity, respectively. The time range is the same as in Fig. 5.

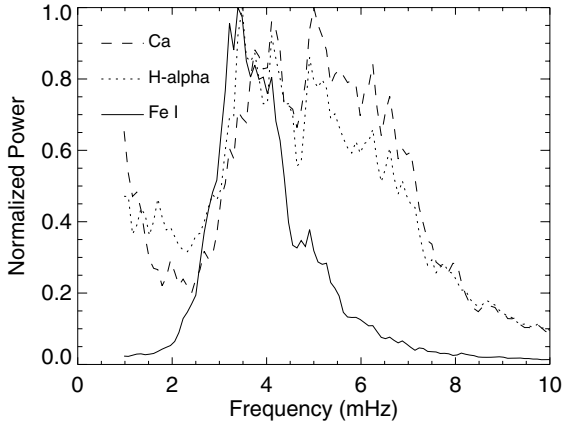

Fig. 8. Power spectrum deduced from the data on 2 August.

correlated with that in Hβ velocity. The cross correlation between Hβ velocity and Ca II H_{2V} intensity oscillatory powers is calculated to be 0.79.

4.2. Data set on 2 August

Similarly, the data obtained on 2 August were analysed. The Hα spectra in the chromosphere were observed on that day instead of Hβ spectra. Figure 8 shows the power spectra as in Fig. 1, although Fig. 8 has better frequency resolution than Fig. 1 because it is deduced from the long duration data set of 150 min. The chromospheric velocity derived from Hα in Fig. 8 indicates stronger power than Hβ in Fig. 1, at the high frequency range of 5–8 mHz. In the Fe I power spectrum, a small enhancement is found at 5 mHz, where strong peaks are denoted in Ca II H_{2V} and Hα.

Figure 9 presents the data where two prominent crests of a wave were found in Ca II H_{2V}. The velocity and excess width in Hα show larger fluctuation than Hβ (see Fig. 3). During the Ca II H_{2V} brightenings, downward velocity peaks in the photosphere precede those in the chromosphere (inferred from Hα) by 30–50 s. The Ca II H_{2V} brightenings coincide with the

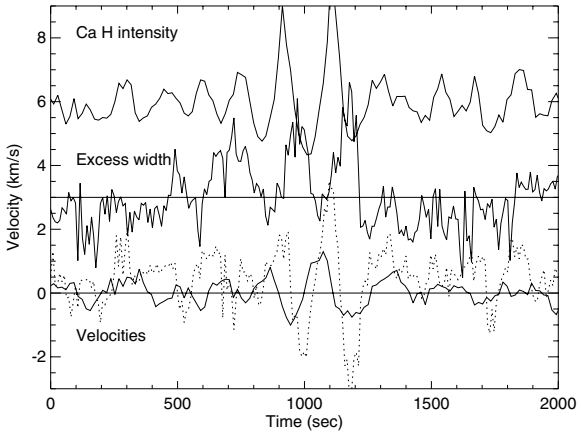

Fig. 9. Time plot of Ca II H_{2V} intensity, Hα excess line width, and velocities. The solid line in the middle indicates the Hα excess line width. Dotted and solid lines in the lower part of the figure are the downward velocities derived from Hα and Fe I. Typical examples of Ca II H_{2V} brightening occur at 910 s and 1100 s. The peaks of Ca II H_{2V} intensity coincide with downward velocities in Hα. The maximum line broadenings of Hα are found just at or shortly before the times of upward velocity peak in Hα.

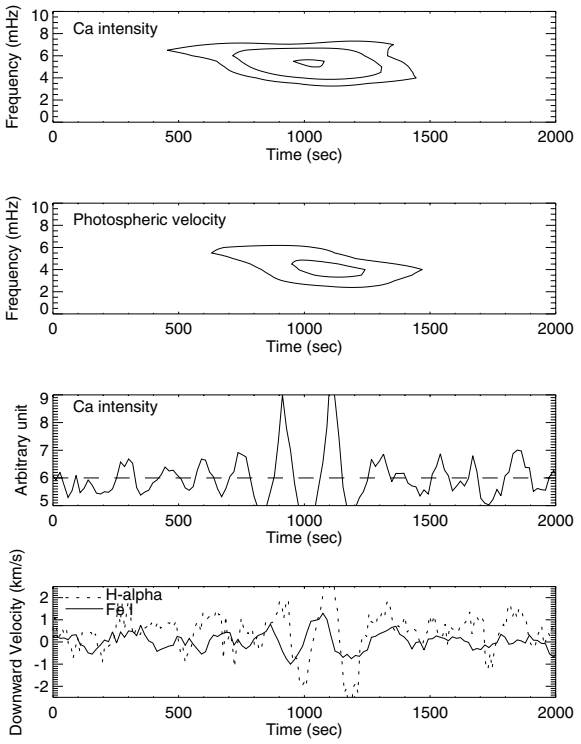

Fig. 10. *Top 2 panels*: contours of power spectra deduced by wavelet transformation of Ca II H_{2V} intensity and photospheric velocity. *Bottom panels*: light curve in Ca II H_{2V}, velocities in Hβ (dotted line), and Fe I (solid line).

downward velocity peak in the chromosphere. The behavior of the Hα excess width during the Ca II H_{2V} brightenings suggests that significant line broadening occurs just at or shortly before the downward velocity peak.

The wavelet analysis of the data in Fig. 9 is presented in Fig. 10. Around the brightening at 1000 s, significant power is detected around 4 mHz in the photosphere. At the same time, Ca II H_{2V} indicates strong oscillatory power around 5 mHz. As the velocity amplitude in the photosphere diminishes, the Ca II H_{2V} intensity oscillation decreases.

Figure 11 displays the photospheric velocity in Fe I. The lower part of the velocity map (0–20 arcsec) is not studied because the spectrum was disturbed by vignetting. Overlaid contours indicate significant power at 5 mHz (cf. Fig. 5).

The velocity in the chromosphere derived from Hα is presented in Fig. 12. Black and white contours mark strong 5 mHz oscillatory power in the photosphere and the chromosphere, respectively. Many of them coincide and the cross correlation between them is 0.42. After 4000 s, a large and long-lasting velocity is found around the position of 90 arcsec where a fragment of the network boundary was located. The pattern of large (5 km s^{-1}) and long duration (300 s) velocity at this part is quite different from the typical 3-min oscillation in the rest of the map. This implies that the strong magnetic flux in the network element influences the behavior of the chromosphere. Long period oscillations may be due to magneto-gravity or MHD waves (McAteer et al. 2002) or to the repeated occurrence of Hα spicules at the network boundary. It is interesting to note that no apparent difference is found in the photospheric velocity at the same location (see Fig. 11).

Figure 13 presents the distribution of Ca II H_{2V} intensity, showing that 5 mHz oscillations in Hα velocity and Ca II H_{2V} intensity are well correlated. The cross correlation between Hα and Ca II H_{2V} oscillatory power is 0.70, which confirms the visual inspection.

5. Discussion

Bright grains in Ca II H_{2V} and K_{2V} are common features in the network cells of the quiet Sun. Previous papers suggest that they are related to 3-min oscillations in the chromosphere (Rutten & Uitenbroek 1991, and references therein). Observed Ca II H_{2V} bright grains are small (2–3 arcsec) and short-lived (1 min) features appearing at 3-min intervals. They are sporadic and localized phenomena in the quiet Sun.

Our results prove that bright grains are indeed associated with enhanced velocity oscillation in the chromosphere. Velocity determination from the Doppler shift of the Ca II H_3 dark core causes ambiguity because it can be affected by brightening or darkening of H_{2V} or H_{2R}. Simultaneous observation of Ca II H and Hα (or Hβ) allows us to establish the relationship between Ca II H_{2V} bright grains and velocity oscillations in the chromosphere. The enhanced Ca II H_{2V} intensity oscillation at 5 mHz, which is the signature of bright grains, is well correlated with the strong 5 mHz velocity oscillation in the chromosphere (Figs. 7 and 13). The cross correlations between 5 mHz oscillatory powers of intensity and velocity are 0.79 and 0.70 for the data sets on 31 July and 2 August.

The numerical simulation by Carlsson & Stein (1997) demonstrated that Ca II H_{2V} bright grains are produced by acoustic shocks propagating upward in the lower chromosphere about 1 Mm above the photosphere. The evolution of Hα velocity and width in Fig. 9 can be interpreted using their model. Downward motion above the shock front and upward motion

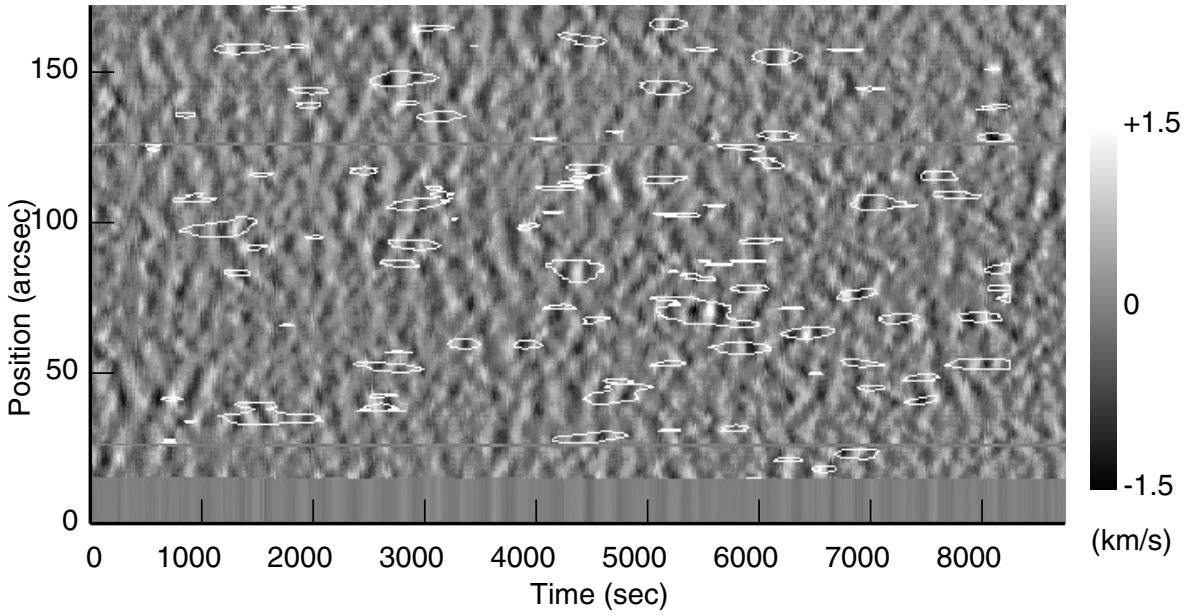

Fig. 11. The evolution of the velocity derived from Fe I. Downward and upward velocities appear bright and dark, respectively. Overlaid white contours indicate significant oscillatory power at 5 mHz.

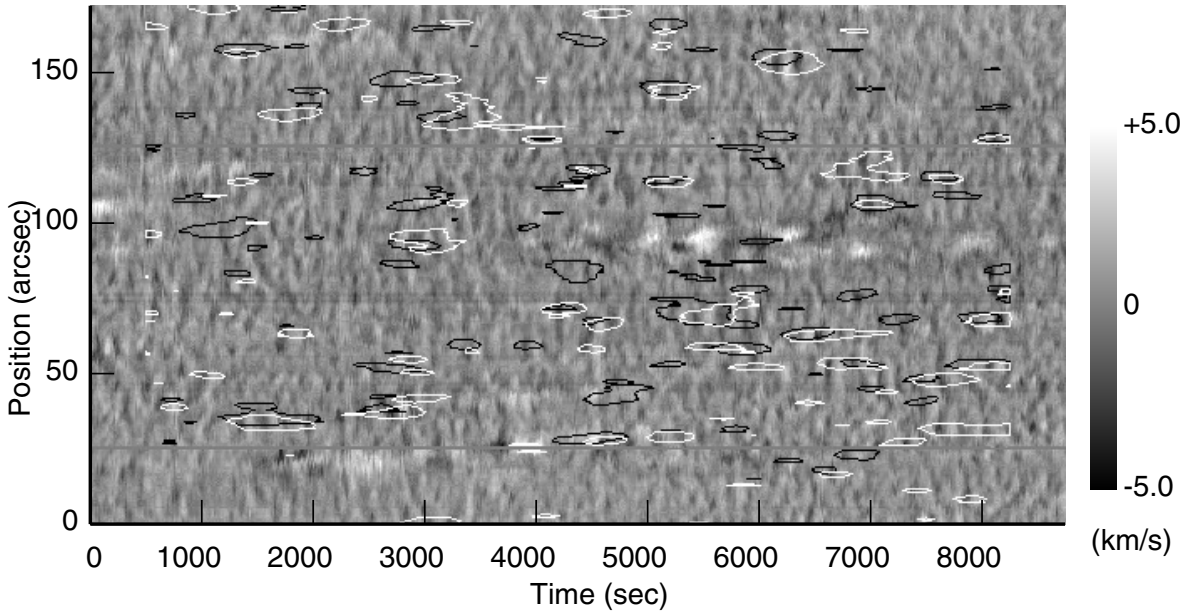

Fig. 12. The evolution of the velocity derived from Hα. White and black contours mark significant 5 mHz power in Hα and in Fe I, respectively. The time range is the same as in Fig. 11.

below it are predicted by the acoustic shock scenario. At first, downward velocity is expected above the shock front in the chromosphere, and then the velocity changes to upward as the shock front moves up in the chromosphere. The large excess width in Fig. 9 increases when the upward velocity increases and attains its maximum. This line broadening suggests the existence of a shock or large velocity gradient in the chromosphere.

Other evidence of acoustic shocks is that the velocity perturbation must propagate with supersonic speed. The time delay between the downward velocity peaks in Fe I and Hα is 30–50 s when bright grains occur (Fig. 9). Assuming that the formation height of the Hα line core is 1.5 Mm above the photosphere (Vernazza et al. 1981), the velocity perturbation must propagate with the mean speed of 30–50 km s^{-1}. Because the sound speed is about 10 km s^{-1} near the photosphere, this suggests the existence of supersonic shocks in association with Ca II H_{2V} bright grains.

At the time of Ca II H_{2V} brightening, the peak downward velocity is found in Hα. This indicates that the peak red-shift of the dark H_3 core in the Ca II H spectra at the time of Ca II H_{2V} brightening (Fig. 2) is a direct result of a large downward velocity in the upper chromosphere. It also agrees with the fact that bright grains are usually found in Ca II H_{2V} and

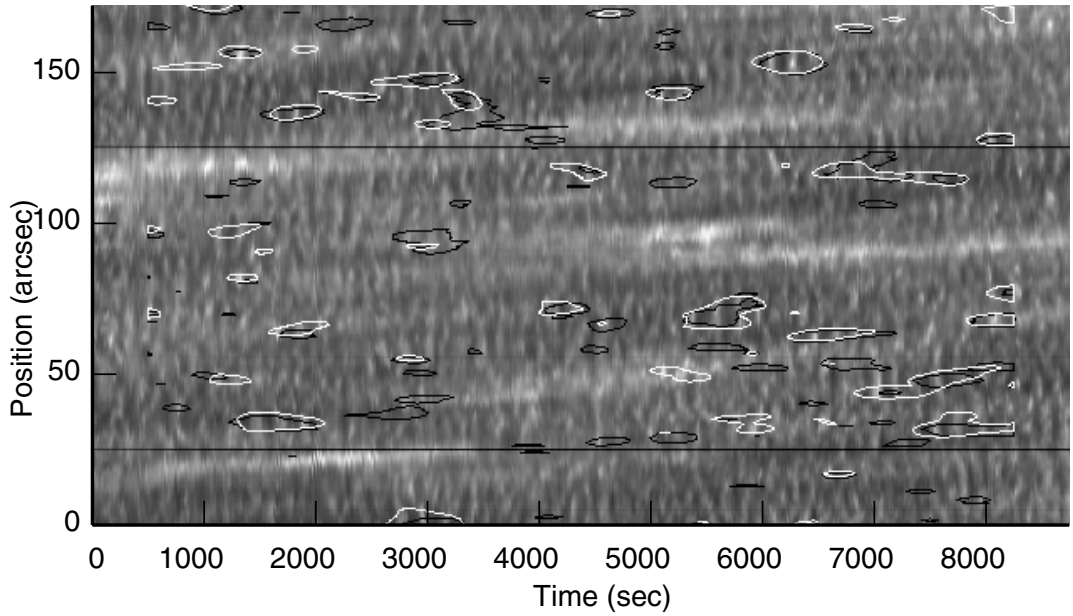

Fig. 13. The evolution of Ca II H_{2V} intensity. White and black contours indicate significant 5 mHz power in Ca II H_{2V} intensity and in Hα velocity, respectively. The time range is the same as in Fig. 11.

Table 1. Cross correlations between oscillatory powers on 31 July.

	Hβ 5 mHz	Ca II H_{2V} 5 mHz
Fe I 3 mHz	0.19	0.14
Fe I 5 mHz	0.57	0.56

Table 2. Cross correlations between oscillatory powers on 2 August.

	Hα 5 mHz	Ca II H_{2V} 5 mHz
Fe I 3 mHz	0.20	0.18
Fe I 5 mHz	0.42	0.48

are less prominent in Ca II H_{2R}. The brightenings are expected to occur both in Ca II H_{2V} and H_{2R}, but the brightening in H_{2R} is absorbed by the overlying red-shifted dark H_3 core (Rutten & Uitenbroek 1991). The velocity of Hβ in Fig. 3 shows the same tendency, but the velocity amplitude is smaller than that of Hα. It reflects the fact that the formation height of Hβ is lower than Hα.

The result of our wavelet transformation revealed that the high frequency (5 mHz) oscillation in the photosphere plays an important role in inducing oscillations of the same frequency in the chromosphere. The power distributions in Figs. 6 and 12 indicate that 5 mHz oscillations in the chromosphere are associated with those in the photosphere. We also examined whether photospheric oscillations at 3 mHz, which is the dominant power in the photosphere (Figs. 1 and 8), is correlated with 5 mHz oscillations in the chromosphere. Tables 1 and 2 present cross correlations between the oscillatory powers at 3 mHz and 5 mHz. The result shows that photospheric oscillations at 5 mHz are more important than oscillations at 3 mHz in connection with the oscillation in the chromosphere, although the frequency of 5 mHz is less prominent in the photosphere. Although Hoekzema et al. (2002) find that excessive Ca II K_{2V} intensity oscillations are associated with 3 mHz acoustic flux with larger-than-random probability, it was far from a one-to-one correlation. Our results clearly indicate the correlation between 5 mHz oscillations in the photosphere and the formation of bright grains. Carlsson & Stein (1997) investigated the relationship between the frequency of photospheric motions and the formation of bright grains by driving the bottom of the atmosphere with motions at different frequency ranges. They concluded that waves near the acoustic cutoff frequency (5 mHz) are crucial in producing bright grains. Their estimation is consistent with our observational results.

Although the Carlsson & Stein (1997) model reproduced the observed characteristics of bright grains, it did not explain the reason grains are localized phenomena, since it was a 1-D simulation. We found bright grains are related to 5 mHz oscillations in the photosphere, and the power distributions in Figs. 5 and 11 indicate that these oscillations are localized and sporadic. Rimmele et al. (1995) derived the spatial distribution of the acoustic flux in the photosphere by using a narrowband filtergram in Fe I (λ543.4 nm). They claimed acoustic events predominantly occur in dark intergranular lanes. Recent 3-D simulations of convection near the photosphere demonstrate that transient acoustic waves are excited when a small granule undergoes a rapid collapse in the intergranular lane (Skartlien et al. 2000; Stein & Nordlund 2001). According to their results, when a granule collapses on a time scale shorter than that of the acoustic cutoff, it causes downflow and leaves a decaying oscillation. They also estimated the occurrence rate of the granule collapse and claim that the process plays an important role in the excitation of 5 mHz waves. It is interesting to note that the typical size of observed grains (2–3 arcsec) is comparable to the size of the collapsing granules. Though

we did not obtain data on the evolution of the granules, it remains a possible excitation mechanism of localized and sporadic waves. This must be examined in future observations.

A remaining question is whether bright grains are correlated with magnetic flux in the internetwork. Schrijver & Title (2003) suggest that the magnetic flux in the internetwork could be connected to the corona. If there is a correlation between bright grains and the magnetic field, grains may play an important role in coronal heating. While magnetic fields are not included in the simulations by Carlsson & Stein (1997) and Skartlien et al. (2000), one possible explanation for the localized nature of grains is that a wave is guided by magnetic flux in the intergranular lanes. Sivaraman & Livingston (1982) claimed a one-to-one correspondence between weak magnetic elements and Ca II K bright points in the internetwork. However, no correlation between the bright grains and magnetic flux has been found in recent observations. Remling et al. (1996) used CN bandhead brightening as a proxy for magnetic flux, but no correlation was found between CN intensity and K_{2V} bright grains. Lites et al. (1999) obtained Ca II H spectrum and polarization data with the Advanced Stokes Polarimeter (ASP), and concluded H_{2V} grains were not correlated with magnetic features. Because internetwork flux concentrations are expected to be small in size (0.1 Mm or less), a higher resolution polarimeter such as the Solar Optical Telescope (SOT) on board Solar-B is required to examine the relationship between magnetic flux and grains in more detail.

6. Conclusions

We observed the quiet Sun with simultaneous spectroscopy in Ca II H, Hα (or Hβ), and Fe I to study the relation between Ca II H_{2V} bright grains and velocity oscillations. We have found typical examples of bright grains, which are short-lived (1 min) brightenings and repeatedly appear at 3-min intervals (Fig. 2). The data sets obtained with multi-line spectroscopy first allowed us to establish the relationship between grain formation and oscillations in the chromosphere and the photosphere. The results indicate Ca II H_{2V} bright grains are clearly associated with enhanced velocity oscillations in the chromosphere. The subsequent Ca II H_{2V} brightenings coincide with maximum downward velocities in the chromosphere, and the line broadening suggests the existence of a velocity gradient or acoustic shock in the chromosphere (Figs. 3 and 9).

Spatial and temporal distributions of oscillatory power are inferred from wavelet transformation. The distribution of 5 mHz power in the photosphere is well correlated with both Ca II H_{2V} intensity and chromospheric velocity. This suggests that Ca II H_{2V} grains are produced by 5 mHz oscillations in the photosphere below. The 3 mHz oscillation, which is prominent in the photosphere, is not important in terms of wave excitation in the chromosphere (Tables 1 and 2). The question of whether or not Ca II H_{2V} bright grains and dark Hα grains are correlated with magnetic flux in the internetwork is very important for the study of coronal heating. We need more detailed observations to solve this problem.

Acknowledgements. Authors would like to thank R. Kitai and S. UeNo for their help in obtaining data at Hida Observatory. We would also like to thank R. Hammer for his helpful comments. We are grateful to G. Attrill for a careful reading of the manuscript. This work is supported by the Grant-in-Aid for the 21st Century COE "Center for Diversity and Universality in Physics" from the Ministry of Education, Culture, Sports, Science and Technology (MEXT) of Japan.

References

Carlsson, M., & Stein, R. F. 1997, ApJ, 481, 500
Cram, L. E., & Damé, L. 1983, ApJ, 272, 355
Gaizauskas, V. 1985, in Chromospheric Diagnostics and Modeling, ed. B. W. Lites (Sunspot, New Mexico: Sacramento Peak Observatory), 25
Hoekzema, N. M., Rimmele, T. R., & Rutten, R. J. 2002, A&A, 390, 681
Kamio, S., & Kurokawa, H. 2004, in proc. SOHO13, Vol. SP-547 (Noordwijk: ESA), 143
Lites, B. W., Rutten, R. J., & Berger, T. E. 1999, ApJ, 517, 1013
McAteer, R. T. J., Gallagher, P. T., Williams, D. R., et al. 2002, ApJ, 567, 165
Remling, B., Deubner, F. L., & Steffens, S. 1996, A&A, 316, 196
Rimmele, T. R., Goode, P. R., Harold, E., & Stebbins, R. T. 1995, ApJ, 444, 119
Rutten, R. J., & Uitenbroek, H. 1991, Sol. Phys., 134, 15
Schrijver, C. J., & Title, A. M. 2003, ApJ, 597, 165
Sivaraman, K. R., & Livingston, W. C. 1982, Sol. Phys., 80, 227
Skartlien, R., Stein, R. F., & Nordlund, Å. 2000, ApJ, 541, 468
Stein, R. F., & Nordlund, Å. 2001, ApJ, 546, 585
Vernazza, J. E., Avrett, E. H., & Loeser, R. 1981, ApJS, 45, 635